Metallomics

Accepted Manuscript

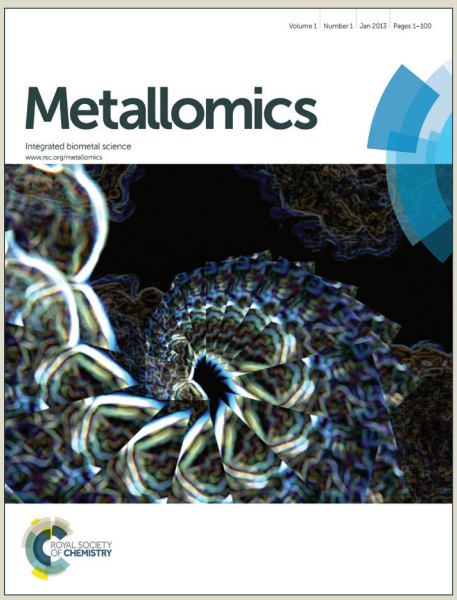

ROYAL SOCIETY OF CHEMISTRY

www.rsc.org/metallomics

Dissolved Cerium contributes to uptake of Ce in presence of differently sized CeO_2-nanoparticles by three crop plants

Franziska Schwabe[a], Simon Tanner[a], Rainer Schulin[a], Aline Rotzetter[b], Wendelin Stark[b], Albrecht von Quadt[c], Bernd Nowack[d]*

a) Soil Protection, Institute of Terrestrial Ecosystems, ETH-Zurich, Universitaetstrasse 16, CH-8092 Zurich, Switzerland

b) Institute for Chemical and Bioengineering, Department of Chemistry and Applied Biosciences, ETH-Zurich, CH-8093 Zurich, Switzerland

c) Institute of Geochemistry and Petrology, Department of Earth Sciences, ETH-Zurich, Clausiusstrasse 25, CH-8092 Zurich, Switzerland

d) Empa-Swiss Federal Laboratories for Materials Science and Technology, Technology & Society Laboratory, Lerchenfeldstrasse 5, CH-9014 St. Gallen, Switzerland

* Corresponding author. Tel.: +41 (0)58 765 76 92

E-mail address: nowack@empa.ch (B. Nowack).

Revised version January 21, 2015

submitted to Metallomics

Abstract

We investigated the uptake of cerium (Ce) dioxide nanoparticles (NP) by hydroponically grown wheat, pumpkin and sunflower plants. The presence of plant roots in nutrient solution led to a substantial increase in the dissolution of CeO_2-NP compared to plant-free medium. Experiments with Zr/CeO_x-NP revealed that Ce was not only taken up in form of NP, but simultaneously to a significant degree also as dissolved Ce(III) ions, which then re-precipitated in form of CeO_2-NP inside the leaves. The contribution of dissolved Ce uptake was particular large for particles smaller than 10 nm due to their higher dissolution rate. Our data also indicate that the translocation of Ce resulting from NP-root-exposure is species dependent. When Ce was supplied as dissolved ions, sunflower had the highest capacity of Ce-ion accumulation inside the leaves, while there was no significant difference between pumpkin and wheat. We found no Ce translocation from roots into shoots when only NPs bigger than 20 nm were applied. This study highlights that plant root activity can have a significant impact on the dissolution of CeO_2 NP in soil solution and that uptake of dissolved Ce(III) followed by re-precipitation needs to be considered as an important pathway in studies of CeO_2-NP uptake by plants.

1. Introduction

The fate and effects of engineered nanoparticles (ENPs) are currently intensely studied by the scientific community. It has been emphasized that uptake and translocation into plants are important aspects to be considered and that beyond toxicity effects in the plants, such exposure may also damage ecosystem functions, biodiversity and crop production[1, 2, 3, 4, 5]. When ENPs are introduced into biological systems, they face a variety of physical and chemical settings that influence their original manufactured features and as a consequence ENPs can undergo transformation reactions[6]. These reactions will affect the reactivity, the fate and the effects of the ENP.

CeO_2 –NPs are of great interest for industrial application due to their capability for undergoing a redox-cycle between the two natural oxidation states (Ce^{3+} and Ce^{4+})[8]. The toxicity of CeO_2-NPs to *E. coli* was found to be linked to the surface speciation of NPs, which was altered in the presence of the bacteria[9]. The toxic effect of CeO_2 to *E. coli* was due to the production of reactive oxygen species (ROS) caused by the redox-cycle between Ce^{3+} and Ce^{4+} on the NP-surface. Adding phosphate to the NP-surface can stop this redox-cycle by trapping Ce^{3+} as $CePO_4$[10].

The incorporation of NP into plant cells requires that they pass through the cell wall, which has pore sizes of maximal 5 nm in most species[11, 12], while passage from roots to shoots through the extracellular space is blocked by the Casparian strip of the root endodermis. Despite these barriers, it has been reported that also NPs larger than 5 nm can be translocated from roots into shoots in some plants, although the results of different studies are controversial, probably due to differences in the tested species, the sizes of nanoparticles and the exposure concentrations[13]. It has also been shown that CeO_2 NP can bypass the Casparian strip in young tissues connecting secondary roots[14].

Only little attention was so far given to possible transformations of CeO_2-NPs. It has been shown recently that cerium dioxide nanoparticles (CeO_2-NPs) are especially prone to transformation reactions in natural and biological system[7]. In this study CeO_2-NPs were added to the rhizosphere of cucumber plants were transformed into $CePO_4$ in the roots and that 21.5% of the Ce found in the leaves had been transformed into Ce carboxylates. Hernandez-Viezcas et al. (2013)[15] found 21% of CeO_2-NPs in soybean nodules in transformed forms. They also reported bio-transformed CeO_2 in soybean pods but the absolute amount was not stated. Zhao et al. (2012)[16] studied biotransformation of CeO_2-NPs in the roots and found different Ce-species, including cerium phosphate. On the other hand, Lopez-Moreno et al. (2010)[17] did not find transformed CeO_2 in the roots of cucumber, alfalfa, tomato and corn seedlings.

CeO_2-NPs were previously thought to be very stable[18] under environmental conditions and therefore have generally been considered as insoluble[19, 20] under environmental conditions. Several studies with these materials have reported only minimal dissolution in a variety of different media with different composition[21, 22]. In an earlier study on CeO_2-NP transformation in plant-free nutrient solution[23] we found that the rate of dissolution varied with media conditions (e.g. reduction or complexation), pH and particle size. From these results we concluded that dissolution depends on the ratio between Ce^{3+} and Ce^{4+} in the NP-surface layer. As NP size decreases, more and more oxygen vacancies occur in the ceria lattice, resulting in local reduction of Ce^{4+}[24]. Following up on the previous study, in which we used plant-free solutions, the aim of the present study was to investigate the role of CeO_2 dissolution in the uptake of Ce from CeO_2 NP suspensions by three commercially important crop plants: sunflower, spring wheat and pumpkin. Using a closed hydroponic exposure system, we exposed 30 d old plants of these three species to suspensions of three differently sized CeO_2 NP groups

(and as control also to an NP-free Ce(III) solution). We determined how dissolved Ce concentrations in the nutrient solution related to Ce accumulation in the roots and shoots of the plants. In an additional experiment plants were exposed to Zr/CeO_x-NPs of 8 nm in diameter in order to enable discrimination between Ce uptake in particulate and dissolved form, based on the Zr:Ce ratios in the shoots of the test plants.

2. Materials and Methods

Nanoparticle manufacturing

Cerium and zirconium-cerium nanoparticles were manufactured as bare/ non-coated NP by flame spray synthesis. Here they are referred to by their mean TEM-diameter size and composition (9 nm CeO_2, 23 nm CeO_2 and 64 nm CeO_2, 8 nm Zr/CeO_x). Sizes represent means determined from TEM-images (100 primary particles per size group).

For synthesis cerium 2-ethylhexanoic acid diluted in xylene (2 wt% for the 9 nm CeO_2-NP and 8 wt% for the 23 nm CeO_2-NP) was used and introduced as a precursor into a methane/oxygen flame[20]. For the 9 nm CeO_2-NPs the flow rate of the precursor was 3 mL min^{-1} (5 mL min^{-1} for the 23 nm CeO_2-NPs), and 7 mL min^{-1} oxygen gas (5 mL min^{-1} for the 23 nm CeO_2-NPs) was used to disperse the liquid leaving a capillary[25]. 64 nm CeO_2-NPs were made from 23 nm CeO_2-NPs by sintering for 16 hours at 700°C[26].

For the production of Zr-CeO_x-NP, 40 g cerium 2-ethylhexanoate diluted in xylene (12.0 wt% Ce) and 38 g zirconium 2-ethylhexanoate (ABCR, 90%) were mixed and subsequently diluted with 150 g toluene. The resulting mixture was introduced as precursor into a methane/oxygen flame. The flow rate of the precursor was 5 mL min^{-1} and 5 mL min^{-1}, oxygen gas was used to disperse the liquid leaving a capillary.

As quality control for each subset the particle size distribution and specific primary particles diameter were determined right after manufacturing, by N_2 adsorption (Brunauer-Emmett-Teller, Micromeritics Tristar 3000), transmission electron microscopy (Tecnai F30 ST, FEI, operated at 300 kV), and X-ray diffraction (X'Pert PRO-MPD, Cu Kα radiation, X'Celerator linear detector system, step size of 0.05°, 45 kV, 40 mA, ambient conditions).

Plant cultivation and treatment

Pumpkin (*Cucurbita maxima*, var. Gelber Zentner) and wheat seeds (*Triticum aestivum* var. Sella) were purchased from UFA-Samen (Fenaco Genossenschaft, Winterthur, Switzerland). Sunflower seeds (*Helianthus annuus* var. Iregi) were acquired from OH-Samen (Rafz, Switzerland). The seeds were washed in deionized (DI) water and then surface sterilized in 6% NaOCl solution for 10 min, rinsed 5 times in DI water and placed on germination paper. Wheat seeds were kept at room temperature (RT) for 4 d in the dark and then for 1 d in light. They were irrigated with DI water and transferred to the hydroponic system 6 d after soaking. Pumpkin and sunflower seeds were kept 5 d in the dark at 28 °C and then 2 d in light at RT. They were also wetted with DI water before being transplanted to the hydroponic system 8 days after soaking. On the hydroponic system, each plant was grown in an individual bottle with 1 L 20% Hoagland solution[27] with the following chemical composition: 800 µmol $Ca(NO_3)_2$, 400 µmol $MgSO_4$, 200 µmol KH_2PO_4, 1 mmol KNO_3, 10 µmol Fe(III)-ETDA, 20 µmol H_3BO_3, 4 µmol $MnSO_4$, 0.4 µmol $ZnSO_4$, 0.4 µmol $CuSO_4$, 0.4 µmol Na_2MoO_4, 10 µmol NaCl, pH adjustment to 5.6 buffered by 5.1 mM MES. All bottles were individually aerated with compressed air and the nutrient solution was replaced every 5 d. These control conditions were kept until plants were 24 d old. Plants were cultivated in an airflow climate-control chamber

(Kälte 3000, Landquart, CH) set to 16 h daylight cycles, 50-60% humidity and 21°C during light periods and 15°C in darkness.

On day 24 the relative chlorophyll content of leaves was measured on 6 spots of each plant (Chlorophyll Meter, SPAD-502, Minolta, Japan). These spots were marked and numbered for repeated measurements on day 30 (Fig. 4-1 points I-IV).

Plants were then exposed for 6 d to the treatment suspensions, while the control groups continued to grow in Hoagland solution without NP-addition. In the treatments with CeO_2 NP, we used 100 mg/L suspensions of CeO_2-NPs dispersed by ultrasonication in 1 L of 20 % Hoagland medium For stabilization gum arabicum (GA) was added at a concentration of 60 mg/L (denoted as "+GA") in one group of replicates, while no GA was added in another (denoted as "pure"). Suspensions of 100 mg/L $ZrCeO_x$-NPs were stabilized by adding GA at a concentration of 90 mg/L.

For the measurement of Ce(III) ion uptake capacity we used 20 % Hoagland solution, buffered at pH 5.8 without addition of any Fe-source or EDTA. Cerium was added in form of 0.1 mM $Ce_2(SO_4)_3$ dissolved in 0.2 mM citric acid and incubated over night on ice. The use of a closed hydroponic system and the treatment of 30 day old plants ensured that leaves, stems and meristems of plants did not come into direct contact with the root-applied NPs. As the solution of the control medium was free from Ce (measurements were always below limits of detection), we concluded that all Ce found in the plant shoots after NP-application to the roots (day 24 ff.) had been translocated from the roots into the shoots. This assumption cannot be made when plant seeds are treated with NPs or when seedlings are germinated in NP containing substrate as in most previous studies, as there is no sufficiently effective methods of NP removal from plant surfaces (e.g. by washing off)[27, 28, 29].

Medium and plant sampling

For the analyses of suspended CeO_2 and particle characterization, samples of 2 mL were taken daily from the top of the medium. Care was taken to avoid resuspension of CeO_2 attached to roots and container walls. Wheat plants transpired around 100 mL, sunflower and pumpkin plants around 250 mL each during the treatment. These losses were recorded and taken into account for concentration calculations. After 29 days of NP exposure, plants were removed from the bottles and divided into roots and shoots (Fig. 4-1- level of section). The shoots were weighed (remaining cotyledons were removed prior to that), dissected and oven dried at 70°C. The roots were rinsed 10 times in DI water, dried with tissues, weighed, and dried at 70°C. After 4 days of drying, the total dry weights of shoots and roots were measured and samples were prepared for analyses.

Primary particle characterization

TEM (transmission electron microscopy) images

Nanoparticle imaging of the synthesized particles was carried out on a CM 12 transmission electron microscope (FEI, Eindhofen, NL) operated at 100 kV. Prior to the measurements, media samples were centrifuged on carbon-coated copper grids following Schwabe et al. (2013)[27].

XRF (X-ray fluorescence) and total carbon content

Elemental analyses of particles were performed by means of XRF (Spectro XEPOS Spectro Analytical Instruments, Germany). After mixing 100 mg of NPs with 3.9 g quartz purum (Fluka, 83340, Switzerland) in a laboratory mill (MM200, Retsch, Switzerland) and homogeneously blending with 0.9 g wax (Cereox by Fluxana, BM-0002-1,

Switzerland) a pellet was pressed at 15 bar for analysis. For the analysis of total carbon content 100 mg of pure NP-samples were heated to 900°C. The resulting CO_2 was quantified using a TOC-L & SSM 5000 A (Shimadzu, Japan). All analyses were performed on three replicate samples.

Particle characterization in suspension and media

The hydrodynamic diameter of the particles (in nm via DLS = dynamic light scattering) and surface charge (zeta-potential) were measured 24 h after ultrasonication in 3 replicates, with 5 measurements each, by a Zetasizer 3000 (Malvern, UK), as follows. The NPs were dispersed at a concentration of 2 g/L CeO_2 in Hoagland medium by ultrasonication (Ultralab 4000, B. Braun, D) at 180 W for 12 min and afterwards diluted to final concentration of 100 mg/LCeO_2–NPs. When GA was added (+ GA) it was supplied before ultrasonication.

The samples taken on day 1, 2, 4 and 6 of treatment were diluted 1:10 in DI water and used to determine particle size distributions by means of nanoparticle tracking analysis (NTA) applied to 40-second videos using a NanoSight LM20, (NanoSight Ltd., Wiltshire, UK). Each sample was analyzed 3 times. The count values between 1 and 500 were summed up in 10 nm clusters and converted to relative intensity (max. value 1). As this method was not capable of tracking NPs > 900 nm, it was not possible to characterize samples without GA-addition for more than two days.

Quantification of cerium

Total Ce in suspensions and media was quantified after digesting samples at 165°C maximum temperature in a microwave oven (lavis Ethos EM-2, MLS GmbH, Germany), first for 60 min in conc. HNO_3 and then for 90 min in 38% H_2O_2, following (Limbach et al., 2008)[30]. After this 2-step digestion procedure, the samples were diluted to 25 mL

with DI-water and analyzed for Ce in 2 ml sub-samples by means of ICP-OES (ICP-OES-MPX, Varian, Switzerland). Shoot Ce contents were analyzed in the same way from 200 mg samples of dried plant material.

Dissolved Ce in the media was quantified after filtering suspensions through 10 kDa Amicon® Ultra-4 Centrifugal Filter (Merck, Millipore, Switzerland) for 30 min at 4300 rpm. The filtered solutions were analyzed by means of ICP-MS after addition of 1% HNO_3. Control media (without NPs) were analyzed in the same way as NP containing suspensions. The limits of detection were 0.2 µg/l for ICP-MS and 0.3 mg/l for ICP-OES.

Quantification of Zr:Ce ratios

Zr/CeO_x-NPs and treated plant samples were HF-digested. 500 mg of ground leaf material was dissolved in HF-acid. At the end the HF-digests were vaporized by heating and neutralized with boric acid and finally re-suspended in HNO_3 to a volume of 500 ml. Also three 20 mg samples of Zr/CeO_x-NPs were HF-digested. Each of these samples was incubated for 5 days at 205 °C with 4 ml HF + 0.5 ml HNO_3 in sealed Teflon digestion bombs. Thereafter, the HF was evaporated on a hot plate, 5 ml of 1 M HCl solution were added, and the bombs were returned to the oven for another 12 h. Finally the solutions were neutralized, NP-digest solutions were diluted 1:2000 with DI-water and analyzed by means of ICP-MS (ICP-MS-920, Varian, CH);

Quantification of total and plant available P

CeO_2-NPs surfaces are known as strong sorbents of PO_4[31]. To quantify the dependence of P binding to NP surfaces in the different particle-size groups we conducted a batch experiment in which samples of CeO_2-NPs were suspended at a concentration of 100 mg/L in 1mM KH_2PO_4 solution and incubated over 7 days on a lab-shaker (pH adjusted to 5 by HCL). For further details on the preparation of the suspensions see Schwabe, et

al. (2014)[23]. On day 7 the particles were allowed to sediment and the upper solution was analyzed for P-content by means of UV-VIS spectrometry at a wavelength of 880 nm (Cary 50, Varian, Inc./Agilent Technologies, Switzerland) using the ammonium molybdate-antimony potassium tartrate-ascorbic acid method of Murphy and Riley (1962)[32]. The same method was used to monitor available P in the plant growth medium. To determine total P in the system 2 ml medium (+/- NPs) samples were taken and analyzed using the 2-step acid digestion method described before followed by ICP-OES (detection limit 0.2 mg/L P).

HPLC for quantification of organic acids

Organic acids in nutrient solution were quantified at the end of the experiment using ion chromatography with conductivity detection on a Metrohm 861 Advanced Compact IC using an AS11 250*4 mm column (Dionex) using 3.2 mM Na_2CO_3 und 1 mM $NaHCO_3$ as mobile phase. The detection limits for citric, malic and tartaric acid were 0.1 mg/L.

STEM-EDX analysis of particles in sunflower leaves

To perform STEM-EDX analysis (Transmission Electron Microscopy coupled with Energy-Dispersive X-ray spectroscopy) 0.4 g leaf samples were taken in the treatments with sunflower. Sunflower was chosen because it showed the highest uptake. The samples were ground and incinerated at 900°C under oxygen-flow, using a TOC-L & SSM 5000 A (Shimadzu, Japan) until the CO_2-peak subsided below detection. The resulting ash was dispersed by means of ultra-sonication in a solution of 200 µl conc. HNO_3 (ultrapure 68%, Fluka, Switzerland), 100 µl Dispex® (BASF, Switzerland) and 15 ml DI water. Ten ml subsamples of the suspension were centrifuged on copper-nickel-grids coated with Formvar® (Science Services GmbH, Germany) at a 90° angle for 300 min at

3000 rpm. The grids were dipped in DI-water and dried prior to STEM-EDX analyses. The following 3 types of samples were prepared in this way: a) ashes of 0.4 g sunflower leaves treated 6 d with Zr/CeO_x-NPs; b) ashes of 0.4 g sunflower leaves treated 6 days with 9 nm CeO_2-NPs without GA; c) ashes of 0.4 g sunflower leaves grown in pure Hoagland without GA and mixed before incineration with 0.5 mg $Ce_2(SO_4)_3$ powder. As control, we also prepared 0.1 mg/L samples of original Zr/CeO_x-NPs dispersed in GA-free Hoagland solution without incineration.

STEM-EDX analysis was carried out using a JEOL JEM 2200fs operated at 200 kV. The nominal spot size of the STEM probe was 0.7 nm using a beam convergence angle of 10.8 mrad. High-angle annular dark-field STEM micrographs were recorded using an inner detector angle of 100 mrad, while the bright-field STEM images were recorded with a detector angle of approximately 15 mrad. EDX spectra of individual particles were recorded either by positioning the electron probe on a selected particle or by scanning the electron probe on a small frame centered on the particle.

Results

Particle characterization

Batches of 9 nm CeO_2 and the 8 nm Zr/CeO_x NP powder showed very similar particle size distributions (SI Fig. 2). In both materials, none out of 100 NPs was larger than 25 nm, while 2% of the Zr/CeO_x particles were even smaller than 4 nm. In the group of 64 nm NPs only 2% of the particles were below 30 nm and no particle was found to be smaller than 20 nm, while some were larger than 100 nm. Particle sizes in the 23 nm group varied between 5 and 60 nm; only 8% were smaller than 10 nm.

After ultra-sonication of NPs in DI-water, the zeta potential increased with decreasing particle size (Table 1). In Hoagland solution and in presence of GA, the zeta potential was negative with only small differences between particle groups. The DLS size measurements indicate that particles agglomerated quickly. Aggregate sizes exceeded 1000 nm in 20% Hoagland medium when no stabilizing agent (GA) was present.

Variation of particle size distributions over time in media with and without plants

The concentration of total Ce remaining in suspension decreased to zero within 2-4 days in all plant treatments without addition of GA (Fig. 2), indicating rapid NP sedimentation. In wheat medium 64 nm NPs disappeared within 4 days also in presence of GA, while some presence was still indicated by low Ce concentrations even after 6 days in the sunflower and pumpkin treatments. The smaller NPs (9 nm and 23 nm) were better retained in suspension. In wheat and sunflower medium 50 mg/L Ce was still found for both the smaller two NP groups after 6 days, which accounts for 67% of the initial Ce concentration, while even higher percentages remained in suspension in the pumpkin treatments (99% for 23 nm NPs, 71% for 9 nm NPs). With all three plants the suspensions of 23 nm NPs appeared to be the most stable, most clearly with pumpkin.

The stabilizing effect of GA on the suspensions is clearly visible in the analyses of particle size distributions using NTA (SI Fig. 4). Also the plant effects on particle/aggregate size distributions largely paralleled those on Ce concentrations in suspension. The smallest agglomerates were found in all media with plants for the 23 nm NP group with a maximum at around 180 nm (SI Fig. 5), in accordance with our previous results[27]. The size of the agglomerates formed by the 9 nm NP group slightly increased over time in sunflower treatment and even more in the pumpkin treatment, while the size distribution tended to shift to smaller diameters in wheat medium. All in all, the 23

nm group showed the most narrow size distributions in Hoagland medium with plant roots

Ce in plant root and shoot samples after the CeO_2 particle treatments

No toxicity effects of the NP treatments were found in root and shoot biomasses or in root:shoot ratios. (Tables S2-S4, Supporting Information) Also chlorophyll content measurements did not indicate any toxicity effects of the applied treatments.

Ce concentrations in plant samples varied strongly with plant species and NP treatment (Fig. 3). In general, Ce concentrations were lower in roots grown in GA-stabilized NP suspensions than in suspensions without GA., Overall sunflower roots seemed to have the lowest affinity to CeO_2. Despite the rather high amounts of Ce bound to wheat roots, no Ce was detected in the shoots of wheat plants exposed to NP, regardless of NP size and GA treatment (Fig. 3A). These results are in accordance with our earlier study[27]. However, when Ce was applied as 0.1 mM Ce(III)-citrate solution, we found 17.2 µg/g Ce in wheat leaves.

Pumpkin and sunflower leaves accumulated more Ce in the Ce(III)-citrate treatment than in the NP treatments. In contrast to wheat, substantial Ce uptake into the leaves of pumpkin and sunflower had occurred in the 9 nm and 23 nm NP treatments, with clearly less uptake from the suspensions with larger particles. No translocation of Ce to the leaves was found in these two species only in the 64 nm NP treatments, which means that there was no significant uptake of particles >20 nm. GA-stabilization decreased the accumulation of Ce in pumpkin leaves from 9.45 µg/g to 5.42 µg/g in the 9 nm NP treatment and from 4.6 µg/g to 0.5 µg/g in the 23 nm NP treatment, while there was no significant GA treatment effect on leaf Ce in sunflower.

In all treatments with detectable Ce uptake sunflower leaves accumulated the highest amounts of Ce, particularly so in the Ce(III)-citrate treatment, indicating that this plant

species has the highest uptake capacity for Ce cations from solution. Within sunflower shoots, Ce concentrations decreased with distance from the roots, i.e. in the order of oldest leaf > stem > apical meristem (SI Fig. 6). A very similar pattern was found in pumpkin (data not shown), in accordance with analogous findings of Zhang et al. (2011)[29] for cucumber, which is a close relative of pumpkin.

Dissolved Ce in hydroponic media

Figure 4 reveals that Ce accumulation in the leaves of the experimental plants showed a rather close relationship to the concentrations of dissolved Ce in the media with NP application (Fig. 4). For wheat, which did not accumulate detectable amounts of Ce in the leaves, the maximum concentration of dissolved Ce was found with 110 µg/L in the 9 nm + GA treatment, whereas up to 500 µg/L dissolved Ce (23 nm pure medium) were measured in pumpkin medium and even 680 µg/L (9 nm + GA medium) in sunflower medium. Dissolved Ce concentrations decreased with increasing NP particle size in parallel with Ce uptake into the leaves. In all cases with detectable Ce accumulation in leaves, the amount of dissolved Ce in the media exceeded the amount of Ce uptake.

While the pH of all hydroponic media was adjusted to 5.6 at the beginning of the experiments, it changed over time and the final pH values varied between 4.6 and 6.4, depending on plant species (SI Tables 3 – 5). Figure 5 shows that the pH appeared to determine the upper limit of dissolved Ce concentrations, as solubility strongly decreased between pH 5.5 and 6.5. Thus the variation in pH may at least partially explain the differences among plant effects on Ce release from NP dissolution. The pH of the medium was not found to be associated with the concentrations of citric, malic and tartaric acid in the hydroponic medium, as their concentrations were always below the detection limit of 0.1 mg/L.

Available P and P-binding to NP-surfaces

As to be expected, the capacity of the CeO_2-NP to adsorb phosphate decreased with increasing particle size in the three NP groups, in accordance with the decrease in specific surface area available for sorption. The 9 nm NP bound 41% of the 200 µM P added to the media, the 23 nm NP 14%, and the 64 nm NP only 4.1%. As a result, different amounts of P remained in solution and were thus available for plant uptake during the 6 days of the experiment in the various NP treatments. In sunflower and pumpkin media the available P was depleted after day 4 of our experiments, whereas in wheat media the available P was only near to depletion in the 9 nm NP-suspensions at day 6 (SI Table 5).

Translocation of 8 nm Zr/CeO_x NP

No dissolved Zr was detected in any of the tested suspensions with Zr/CeO_x particles. Even after a conc. HNO_3 acid digestion, no dissolved Zr was measured, in agreement with the assumption that the Zr-backbone of these particles was virtually indestructible. While the particles were composed of equal molar amounts of cerium and zirconium, corresponding to a Ce:Zr mass ratio of 1:2, all leaves from plants exposed to suspensions containing these particles showed Ce:Zr mass ratios larger than 1:2 (Fig. 6A), except for one pumpkin plant with a leaf Ce:Zr ratio of 1:2. The medium of this plant was particular among all plants in having an exceptionally high medium pH of 7.5 and thus a very low concentration (3 µg/L) of dissolved Ce. In all other cases the concentration of dissolved Ce in the medium was higher than 50 µg/L (Fig. 6B).

Using the Zr:Ce ratio of the initial NPs and the one measured inside the leafs allows us to calculate the percentage of Ce taken up in dissolved form. This percentage was 60%,

75% and 82% in the three sunflower leaves and 78%, 86% and 0% in the three pumpkin leaves that were analyzed

STEM-EDX analysis of Ce in Zr/CeO_x treated sunflower leaf samples

In the Zr/CeO_x treated sunflower leaf samples, particles of different sizes, some also bigger than 20 nm, and diverse shapes were found in the leaf samples of the sunflower plants that had been grown on NP-containing medium (Fig. 7). All EDX spectra of particles visible on the TEM grids revealed the presence of Ce, many also provided clear evidence for the presence of Zr, as for example the particle shown in Fig. 7B.

The Zr-containing particles had a very similar shape as the primary particles applied to the nutrient solution. Their crystal structure and defined rhombic form are typical for NP generated by flame spray synthesis[20]. In contrast, no Zr was found in other particles with totally different shapes, many of which were much larger than the maximum size (25 nm) of the Zr/Ce-NP (Fig. 7C). These Zr-free particles were very similar in shape and size to the particles found in the samples to which $Ce_2(SO_4)_3$ had been added during sample preparation (SI Fig. 7b), suggesting that they had formed in the plant from dissolved Ce, either already during the experiment or afterwards as result of the sample preparation procedure. No Zr was detected in any of the sunflower leaf samples from the treatments with no application of Zr/CeO_x-NP.

Discussion

The low rates of Ce translocation from plant roots into shoots in our study are in agreement with the findings reported in other publications[11, 33, 34], including our previous study[27]. Only Wang et al. (2013)[35] reported very high root-to-shoot translocation of Ce in tomato plants grown in hydroponics containing CeO_2-NP. They

found 1200 µg/g DW of Ce in leaves and 1600 µg/g Ce in roots. In general, it was found that concentrations of NP were about 100 times higher in the roots than in the leaves of a plant[2, 36, 37, 38].

CeO_2-NPs were usually considered as essentially insoluble in studies of NP uptake by plants[13, 37]. Consequently, any translocation of Ce into aboveground plant parts was interpreted as evidence for uptake of NP. However, our results clearly show that CeO_2-NPs dissolved in nutrient solution and generated dissolved Ce concentrations of up to 680 µg/L, depending on NP size, solution pH, presence of stabilizing agents such as GA, phosphorus binding to NP-surface and other factors potentially influencing CeO_2-NP dissolution.

Proton release and excretion of small organic acids e.g. citrate and oxalate[39] from roots can result in substantial rhizosphere acidification. Citrate is one of the most prominent root exudates and also known to dissolve Ce from $CePO_4$ in rocks (monazite) as efficient as EDTA[40]. The measured concentrations of citrate and other organic acids were rather low (lower than 0.1 mg/l) in our study. But this does not necessarily mean that they played no role in CeO_2-NP dissolution. It is well known that low-molecular-weight organic acids are rapidly metabolized by microorganisms in rhizosphere solutions[41], and their influence on CeO_2-NPs uptake and toxicity has been shown in a previous study, with coated particles having less toxicity[42].

The reaction of CeO_2-NPs with PO_4 present in nutrient solution can lead to the formation of insoluble $CePO_4$. This needs to be considered in plant/NP studies[31, 43]. According to speciation calculations no measurable concentration of dissolved Ce should be expected in the presence of PO_4[23]. Nonetheless, we detected dissolved Ce at the end of our experiments. We assume that binding of PO_4 to the NPs indeed decreased Ce solubility initially, but that the phosphate in solution was subsequently depleted through plant

uptake, resulting in the re-dissolution of the $CePO_4$ precipitates and the release of Ce into the plant medium.

The presence of dissolved Ce in the medium means that uptake of dissolved Ce and possible re-precipitation inside the plants have to be considered[11, 44, 45]. Thus, we hypothesized that at least part of the Ce found inside the plants had been taken up and translocated in the plants as dissolved Ce(III). However, the finding of Zr/Ce particles in the leave samples provides clear evidence that there was also uptake and translocation of Ce in form of particles, since the Zr found in the leaves could only have been transported in form of these particles.

The fact that more Ce was found in the leaves of plants exposed to Zr/CeO_x-NPs than expected based on the Zr:Ce ratio of these NPs indicates that in addition some Ce was taken up in non-NP form, with percentages of dissolved Ce contribution of up to 86%. Although the dissolution of Ce from the Zr/CeO_x particles in the nutrient solution was small (0.9% of the added Ce), this concentration was high enough to change the Zr:Ce-ratio significantly inside the plant and result in particulate forms of Ce detectable by STEM. The surface charge and the primary particle sizes of the Zr/CeO_x-NPs and the 9 nm CeO_2-NPs were very similar in Hoagland medium. Thus, due to their insoluble Zr-backbone, Zr/CeO_x-NPs may be used as a non-dissolvable proxy in studying the role of particles in plant uptake of Ce or other processes, in which dissolution of CeO_2 cannot be excluded.

Our STEM analysis of the NPs extracted from leaves revealed two different kind of particles: Zr/Ce-containing particles with about 10 nm diameter, representative of the original Zr/Ce particles, and larger particles of different shapes, which contained Ce, but no Zr and no phosphorus. Biotransformed $CePO_4$ particles were described as needle-like particles[7]. We did not detect such structures in the TEM images. Based on the STEM-EDX

results of the Ce-powder control experiment, we suggest that the particles containing only Ce were formed from Ce-ions in the leaves during sample incineration.

In conclusion, our results show that some plants such as pumpkin and sunflower can take up Ce in form of NP, but that – in contrast to the generally accepted notion – finding Ce in plants does not necessarily imply uptake in form of NP, even when Ce is supplied only in form of NP. A more careful evaluation of claims of NP-uptake by plants is therefore clearly needed because particle and dissolved ion uptake may occur simultaneously

Acknowledgement

We kindly acknowledge Dr. Thomas Bucheli and Alexander Gogos from Agroscope Reckenholz-Tänikon (ART) for their support in DLS and zeta potential measurements. We appreciate the outstanding help and hard work with the plant samples of Evelyne Kieser and Anja Sutter. We thank Dr. Susan Tandy for editing the manuscript. Financial support by ETH Zurich (ETHIIRA Project, ETH- 21 08-3) is kindly acknowledged.

References

1. Petersen, E. J.; Henry, T. B.; Zhao, J.; MacCuspie, R. I.; Kirschling, T. L.; Dobrovolskaia, M. A.; Hackley, V.; Xing, B.; White, J. C., Identification and avoidance of potential artifacts and misinterpretations in nanomaterial ecotoxicity measurements. *Environ Sci Technol* **2014,** *48*, (8), 4226-46.
2. Gardea-Torresdey, J. L.; Rico, C. M.; White, J. C., Trophic Transfer, Transformation, and Impact of Engineered Nanomaterials in Terrestrial Environments. *Environmental Science & Technology* **2014,** *48*, (5), 2526-2540.
3. Lowry, G. V.; Hotze, E. M.; Bernhardt, E. S.; Dionysiou, D. D.; Pedersen, J. A.; Wiesner, M. R.; Xing, B. S., Environmental Occurrences, Behavior, Fate, and Ecological Effects of Nanomaterials: An Introduction to the Special Series. *J Environ Qual* **2010,** *39*, (6), 1867-1874.
4. Batley, G. E.; Kirby, J. K.; McLaughlin, M. J., Fate and Risks of Nanomaterials in Aquatic and Terrestrial Environments. *Accounts Chem Res* **2013,** *46*, (3), 854-862.
5. Zhao, L. J.; Sun, Y. P.; Hernandez-Viezcas, J. A.; Servin, A. D.; Hong, J.; Niu, G. H.; Peralta-Videa, J. R.; Duarte-Gardea, M.; Gardea-Torresdey, J. L., Influence of CeO2 and ZnO Nanoparticles on Cucumber Physiological Markers and Bioaccumulation of Ce and Zn: A Life Cycle Study. *J Agr Food Chem* **2013,** *61*, (49), 11945-11951.
6. Wang, B.; Feng, W.; Zhao, Y.; Chai, Z., Metallomics insights for in vivo studies of metal based nanomaterials. *Metallomics* **2013,** *5*, (7), 793-803.
7. Zhang, P.; Ma, Y. H.; Zhang, Z. Y.; He, X.; Zhang, J.; Guo, Z.; Tai, R. Z.; Zhao, Y. L.; Chai, Z. F., Biotransformation of Ceria Nanoparticles in Cucumber Plants. *Acs Nano* **2012,** *6*, (11), 9943-9950.
8. Cassee, F. R.; van Balen, E. C.; Singh, C.; Green, D.; Muijser, H.; Weinstein, J.; Dreher, K., Exposure, Health and Ecological Effects Review of Engineered Nanoscale Cerium and Cerium Oxide Associated with its Use as a Fuel Additive. *Crit Rev Toxicol* **2011,** *41*, (3), 213-229.
9. Thill, A.; Zeyons, O.; Spalla, O.; Chauvat, F.; Rose, J.; Auffan, M.; Flank, A. M., Cytotoxicity of CeO_2 nanoparticles for Escherichia coli. Physico-chemical insight of the cytotoxicity mechanism. *Environ. Sci. Technol.* **2006,** *40*, 6151-6156.
10. Singh, S.; Dosani, T.; Karakoti, A. S.; Kumar, A.; Seal, S.; Self, W. T., A phosphate-dependent shift in redox state of cerium oxide nanoparticles and its effects on catalytic properties. *Biomaterials* **2011,** *32*, (28), 6745-53.
11. Miralles, P.; Church, T. L.; Harris, A. T., Toxicity, Uptake, and Translocation of Engineered Nanomaterials in Vascular plants. *Environ Sci Technol* **2012,** *46*, (17), 9224-9239.
12. Fleischer, A.; O'Neill, M. A.; Ehwald, R., The pore size of non-graminaceous plant cell walls is rapidly decreased by borate ester cross-linking of the pectic polysaccharide rhamnogalacturonan II. *Plant Physiol* **1999,** *121*, (3), 829-838.
13. Rico, C. M.; Majumdar, S.; Duarte-Gardea, M.; Peralta-Videa, J. R.; Gardea-Torresdey, J. L., Interaction of Nanoparticles with Edible Plants and Their Possible Implications in the Food Chain. *Journal of Agricultural and Food Chemistry* **2011,** *59*, (8), 3485-3498.
14. Majumdar, S.; Peralta-Videa, J. R.; Bandyopadhyay, S.; Castillo-Michel, H.; Hernandez-Viezcas, J.-A.; Sahi, S.; Gardea-Torresdey, J. L., Exposure of cerium oxide nanoparticles to kidney bean shows disturbance in the plant defense mechanisms. *Journal of Hazardous Materials* **2014,** *278*, (0), 279-287.
15. Hernandez-Viezcas, J. A.; Castillo-Michel, H.; Andrews, J. C.; Cotte, M.; Rico, C.; Peralta-Videa, J. R.; Ge, Y.; Priester, J. H.; Holden, P. A.; Gardea-Torresdey, J. L., In Situ

Synchrotron X-ray Fluorescence Mapping and Speciation of CeO2 and ZnO Nanoparticles in Soil Cultivated Soybean (Glycine max). *Acs Nano* **2013,** *7*, (2), 1415-1423.
16. Zhao, L. J.; Peralta-Videa, J. R.; Varela-Ramirez, A.; Castillo-Michel, H.; Li, C. Q.; Zhang, J. Y.; Aguilera, R. J.; Keller, A. A.; Gardea-Torresdey, J. L., Effect of surface coating and organic matter on the uptake of CeO2 NPs by corn plants grown in soil: Insight into the uptake mechanism. *J Hazard Mater* **2012,** *225*, 131-138.
17. Lopez-Moreno, M. L.; de la Rosa, G.; Hernandez-Viezcas, J. A.; Peralta-Videa, J. R.; Gardea-Torresdey, J. L., X-ray absorption spectroscopy (XAS) corroboration of the uptake and storage of CeO(2) nanoparticles and assessment of their differential toxicity in four edible plant species. *J Agr Food Chem* **2010,** *58*, (6), 3689-93.
18. Walser, T.; Limbach, L. K.; Brogioli, R.; Erismann, E.; Flamigni, L.; Hattendorf, B.; Juchli, M.; Krumeich, F.; Ludwig, C.; Prikopsky, K.; Rossier, M.; Saner, D.; Sigg, A.; Hellweg, S.; Gunther, D.; Stark, W. J., Persistence of engineered nanoparticles in a municipal solid-waste incineration plant. *Nat Nanotechnol* **2012,** *7*, (8), 520-524.
19. Rico, C. M.; Hong, J.; Morales, M. I.; Zhao, L.; Barrios, A. C.; Zhang, J. Y.; Peralta-Videa, J. R.; Gardea-Torresdey, J. L., Effect of cerium oxide nanoparticles on rice: a study involving the antioxidant defense system and in vivo fluorescence imaging. *Environ Sci Technol* **2013,** *47*, (11), 5635-42.
20. Madler, L.; Stark, W. J.; Pratsinis, S. E., Flame-made ceria nanoparticles. *J Mater Res* **2002,** *17*, (6), 1356-1362.
21. Cornelis, G. C. G.; Ryan, B.; McLaughlin, M. J.; Kirby, J. K.; Beak, D.; Chittleborough, D., Solubility and Batch Retention of CeO(2) Nanoparticles in Soils. *Environmental Science & Technology* **2011,** *45*, (7), 2777-2782.
22. Röhder, L. A.; Brandt, T.; Sigg, L.; Behra, R., Influence of agglomeration of cerium oxide nanoparticles and speciation of cerium(III) on short term effects to the green algae Chlamydomonas reinhardtii. *Aquatic Toxicology* **2014,** *152*, (0), 121-130.
23. Schwabe, F.; Schulin, R.; Rupper, P.; Rotzetter, A.; Stark, W. J.; Nowack, B., Dissolution and transformation of cerium oxide nanoparticles in plant growth media. *accepted by Journal of nanoparticle research* **2014**.
24. Karakoti, A. S.; Munusamy, P.; Hostetler, K.; Kodali, V.; Kuchibhatla, S.; Orr, G.; Pounds, J. G.; Teeguarden, J. G.; Thrall, B. D.; Baer, D. R., Preparation and characterization challenges to understanding environmental and biological impacts of ceria nanoparticles. *Surface and Interface Analysis* **2012,** *44*, (8), 882-889.
25. Stark, W. J.; Madler, L.; Maciejewski, M.; Pratsinis, S. E.; Baiker, A., Flame synthesis of nanocrystalline ceria-zirconia: effect of carrier liquid. *Chemical Communications* **2003**, (5), 588-589.
26. Limbach, L. K.; Li, Y. C.; Grass, R. N.; Brunner, T. J.; Hintermann, M. A.; Muller, M.; Gunther, D.; Stark, W. J., Oxide nanoparticle uptake in human lung fibroblasts: Effects of particle size, agglomeration, and diffusion at low concentrations. *Environmental science & technology* **2005,** *39*, (23), 9370-9376.
27. Schwabe, F.; Schulin, R.; Limbach, L. K.; Stark, W.; Burge, D.; Nowack, B., Influence of two types of organic matter on interaction of CeO2 nanoparticles with plants in hydroponic culture. *Chemosphere* **2013,** *91*, (4), 512-20.
28. Birbaum, K.; Brogioli, R.; Schellenberg, M.; Martinoia, E.; Stark, W. J.; Gunther, D.; Limbach, L. K., No Evidence for Cerium Dioxide Nanoparticle Translocation in Maize Plants. *Environmental Science & Technology* **2010,** *44*, (22), 8718-8723.
29. Zhang, Z. Y.; He, X.; Zhang, H. F.; Ma, Y. H.; Zhang, P.; Ding, Y. Y.; Zhao, Y. L., Uptake and distribution of ceria nanoparticles in cucumber plants. *Metallomics* **2011,** *3*, (8), 816-822.

30. Limbach, L. K.; Bereiter, R.; Müller, E.; Krebs, R.; Gälli, R.; Stark, W. J., Removal of oxide nanoparticles in a model wastewater treatment plant: Influence of agglomeration and surfactants on clearing efficiency. *Environ. Sci. Technol.* **2008,** *42*, (15), 5828-5833.
31. Recillas, S.; Garcia, A.; Gonzalez, E.; Casals, E.; Puntes, V.; Sanchez, A.; Font, X., Preliminary study of phosphate adsorption onto cerium oxide nanoparticles for use in water purification; nanoparticles synthesis and characterization. *Water Sci Technol* **2012,** *66*, (3), 503-509.
32. Murphy, J.; Riley, J. P., A Modified Single Solution Method for Determination of Phosphate in Natural Waters. *Anal Chim Acta* **1962,** *26*, (1), 31-&.
33. Wang, Q.; Ma, X. M.; Zhang, W.; Pei, H. C.; Chen, Y. S., The impact of cerium oxide nanoparticles on tomato (Solanum lycopersicum L.) and its implications for food safety. *Metallomics* **2012,** *4*, (10), 1105-1112.
34. Morales, M. I.; Rico, C. M.; Hernandez-Viezcas, J. A.; Nunez, J. E.; Barrios, A. C.; Tafoya, A.; Flores-Marges, J. P.; Peralta-Videa, J. R.; Gardea-Torresdey, J. L., Toxicity Assessment of Cerium Oxide Nanoparticles in Cilantro (Coriandrum sativum L.) Plants Grown in Organic Soil. *J Agric Food Chem* **2013,** *61*, (26), 6224-30.
35. Wang, Q.; Ebbs, S. D.; Chen, Y. S.; Ma, X. M., Trans-generational impact of cerium oxide nanoparticles on tomato plants. *Metallomics* **2013,** *5*, (6), 753-759.
36. Dietz, K. J.; Herth, S., Plant nanotoxicology. *Trends in Plant Science* **2011,** *16*, (11), 582-589.
37. Lopez-Moreno, M. L.; de la Rosa, G.; Hernandez-Viezcas, J. A.; Castillo-Michel, H.; Botez, C. E.; Peralta-Videa, J. R.; Gardea-Torresdey, J. L., Evidence of the Differential Biotransformation and Genotoxicity of ZnO and CeO2 Nanoparticles on Soybean (Glycine max) Plants. *Environmental Science & Technology* **2010,** *44*, (19), 7315-7320.
38. Zhu, H.; Han, J.; Xiao, J. Q.; Jin, Y., Uptake, translocation, and accumulation of manufactured iron oxide nanoparticles by pumpkin plants. *J. Environ. Monitoring* **2008,** *10*, 713-717.
39. Jones, D. L., Organic acids in the rhizosphere - a critical review. *Plant Soil* **1998,** *205*, (1), 25-44.
40. Cervini-Silva, J.; Fowle, D. A.; Banfield, J., Biogenic dissolution of a soil cerium-phosphate mineral. *Am J Sci* **2005,** *305*, (6-8), 711-726.
41. Kuzyakov, Y.; Raskatov, A.; Kaupenjohann, M., Turnover and distribution of root exudates of Zea mays. *Plant Soil* **2003,** *254*, (2), 317-327.
42. Trujillo-Reyes, J.; Vilchis-Nestor, A. R.; Majumdar, S.; Peralta-Videa, J. R.; Gardea-Torresdey, J. L., Citric acid modifies surface properties of commercial CeO2 nanoparticles reducing their toxicity and cerium uptake in radish (Raphanus sativus) seedlings. *J Hazard Mater* **2013,** *263*, 677-684.
43. Abel, S.; Ticconi, C. A.; Delatorre, C. A., Phosphate sensing in higher plants. *Physiol Plantarum* **2002,** *115*, (1), 1-8.
44. Kumar, V.; Yadav, S. K., Plant-mediated synthesis of silver and gold nanoparticles and their applications. *Journal of Chemical Technology and Biotechnology* **2009,** *84*, (2), 151-157.
45. Sharma, N. C.; Sahi, S. V.; Nath, S.; Parsons, J. G.; Gardea-Torresdey, J. L.; Pal, T., Synthesis of plant-mediated gold nanoparticles and catalytic role of biomatrix-embedded nanomaterials. *Environ. Sci. Technol.* **2007,** *41*, (14), 5137-5142.

Figures and Tables

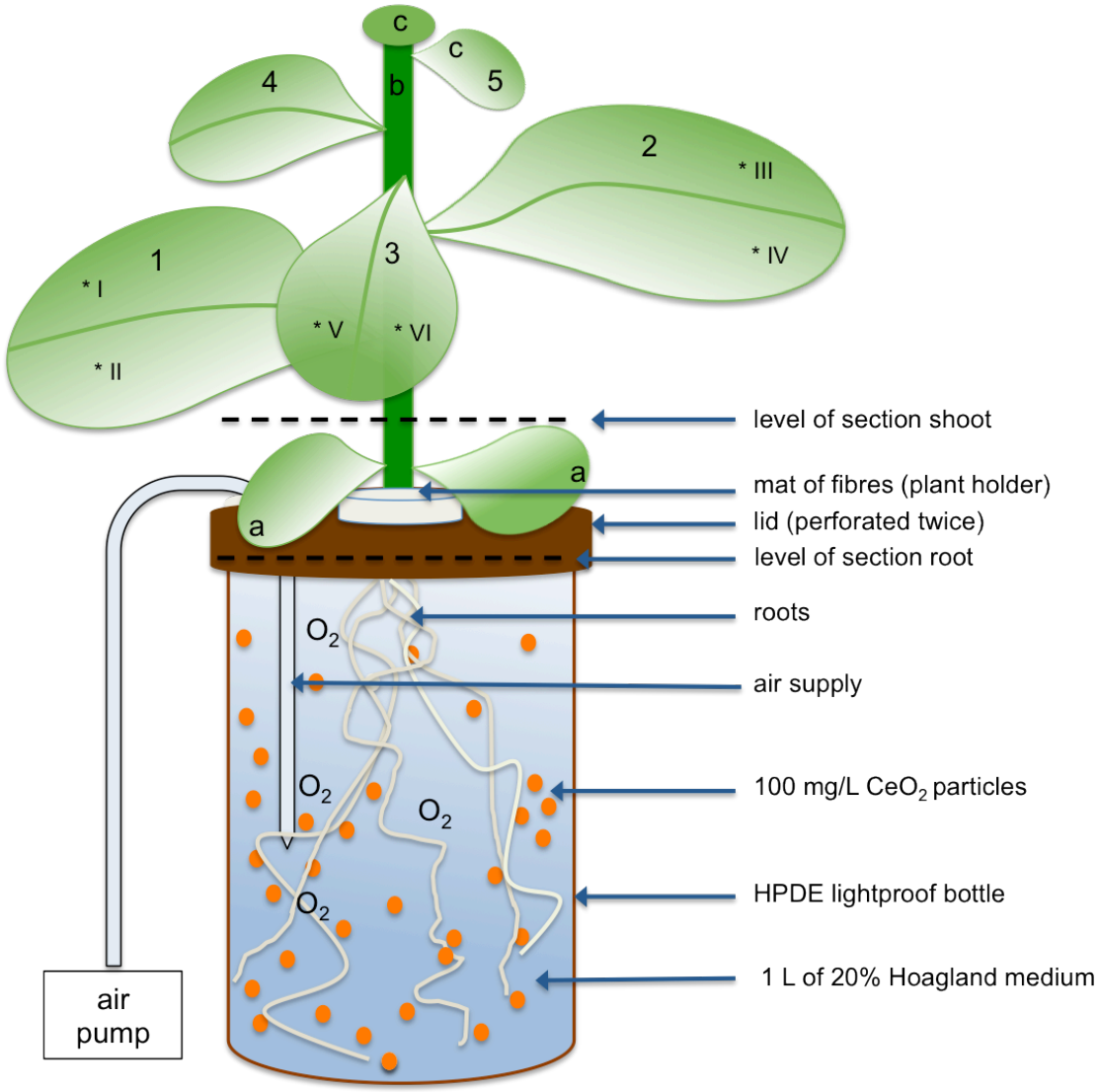

*Fig. 1 Scheme of the experimental set up for one hydroponically cultivated plant. Labeling: a) cotyledons – were removed before harvest; b) stem; c) meristem incl. newest leaf not older than 7 d; 1-5) leaf count; *I- *VI) marked point for chlorophyll measurements*

Table 1: Particle characterization in different suspensions, measured 24 h after ultrasonication, DLS= dynamic light scattering. N=4, each replicated was measured 5 times

Dispersion	**DLS-Size (nm)**							
	CeO_2 9 nm	STDV	CeO_2 23 nm	STDV	CeO_2 64 nm	STDV	Zr/CeOx 8 nm	STDV
Millipore	140	0	145	0	262	4	184	2
Millipore + GA	274	3	177	6	257	0	149	2
20% Hoagland pH 5.6 + GA	184	2	161	3	239	2	147	1
20% Hoagland pH 5.6 (- GA)	3023	263	3566	887	11852	6333	n.a.	
	Zetapotential (mV)							
Millipore	44.9	1	22.1	1	7.4	0	42.7	1
Millipore + GA	-24.7	0	-24.3	1	-21.3	0	-31.5	0
20% Hoagland pH 5.6	-16.8	1	-16.4	1	-26.6	0	-18.1	0
20% Hoagland pH 5.6 (-GA)	-16.2	1	-16.9	1	-20.8	3	n.a.	

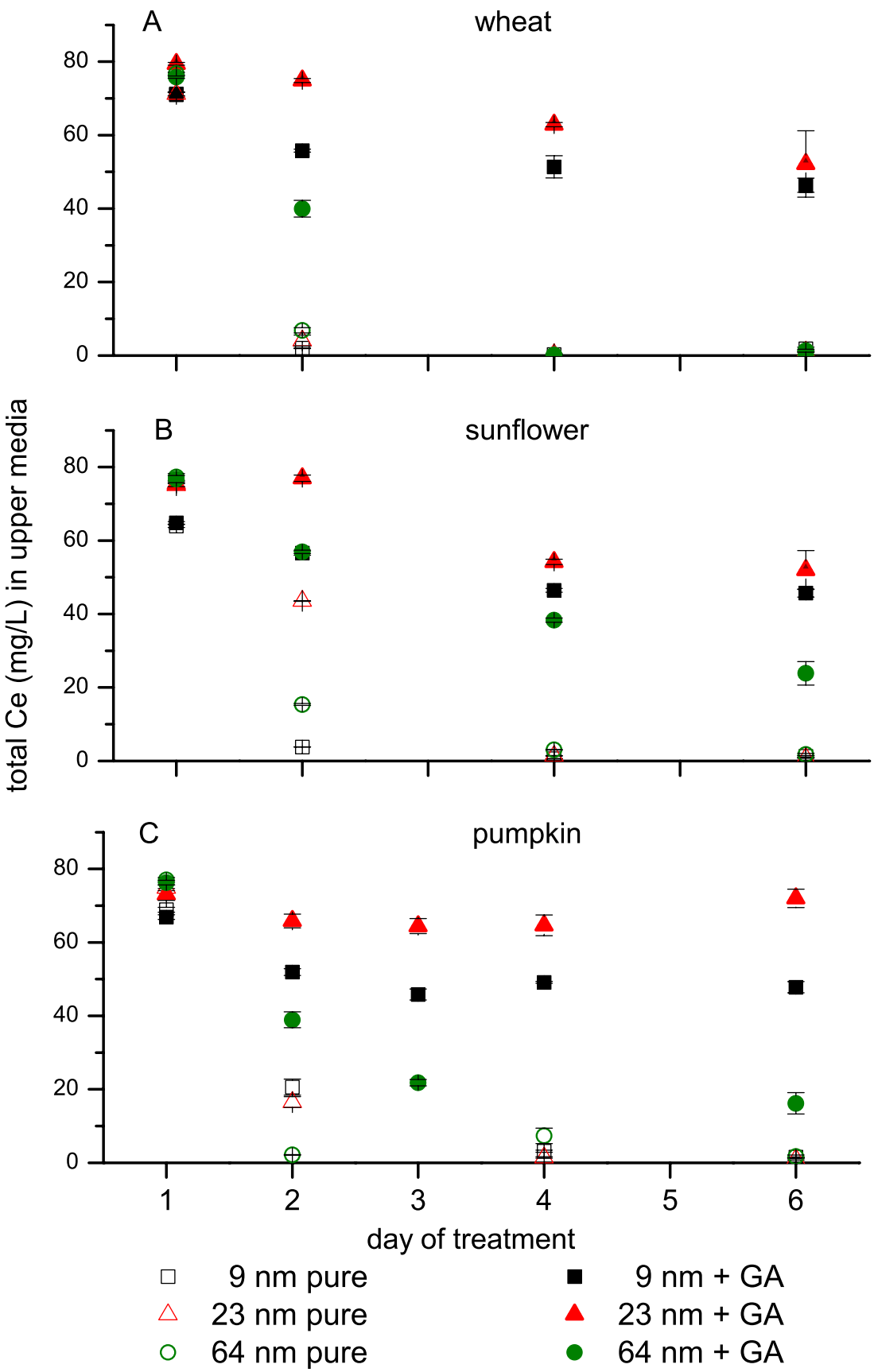

Fig. 2 Total Ce-concentration in suspension during plant exposure with wheat, sunflower and pumpkin. Comparison of the different NP-groups in respect to plant-species grown on the suspension. Initial Ce was 84 mg/l.

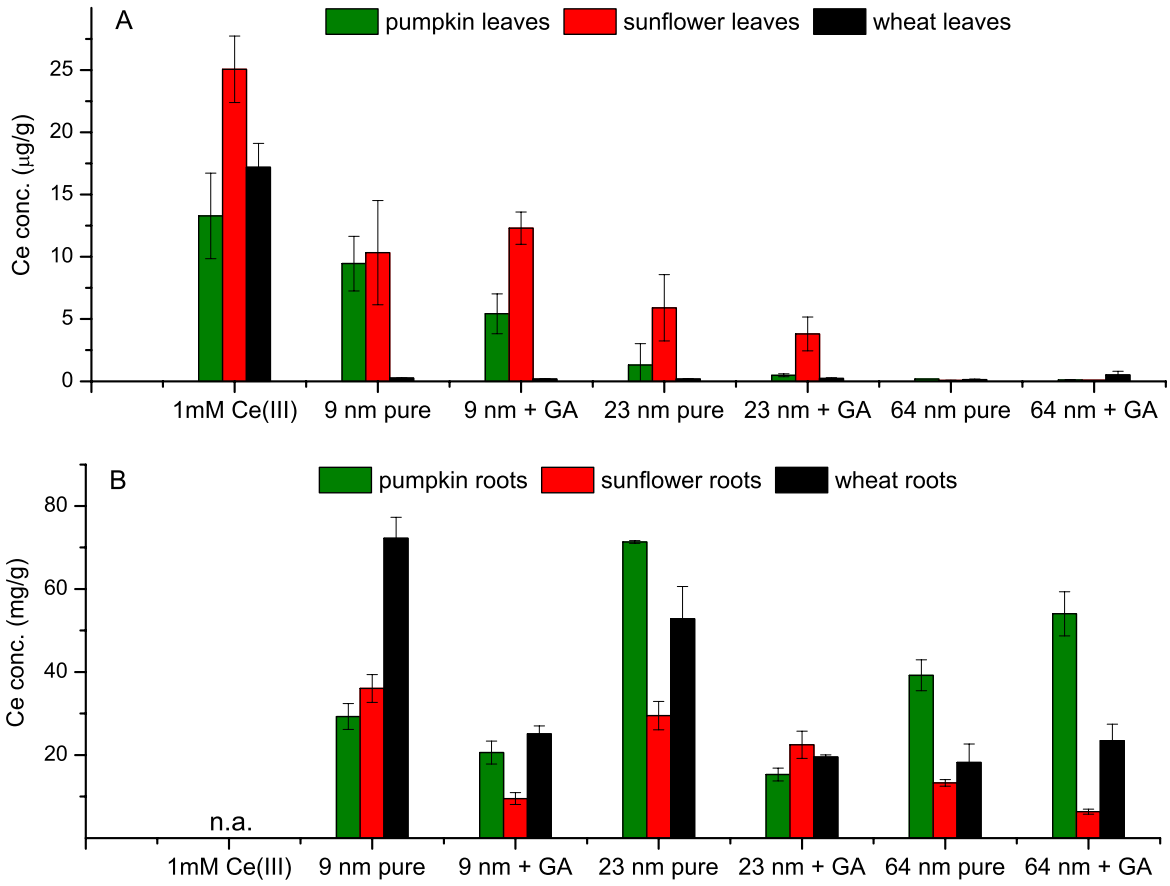

Fig. 3 Ce-concentration found in plant parts after hydroponic exposure of dissolved Ce(III) and particulate CeO_2 in three sizes. A) Ce in leaves; B) Ce-concentration in and on roots after rinsing 10 times with DI-water. Controls are not shown since values were below the detection limit of 0.2 µg/g. GA: Gum Arabic that was used as dispersing agent.

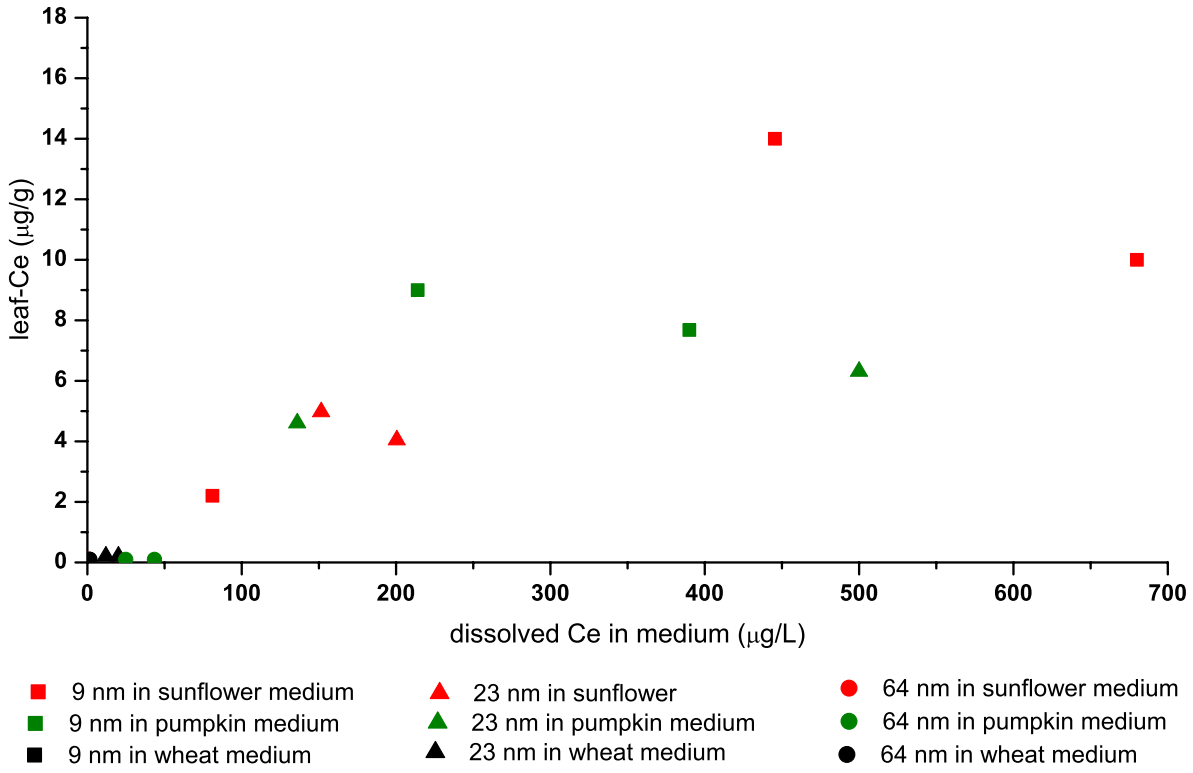

Fig. 4 Concentration of dissolved Ce in plant-growth medium at the end of the experiment (x-axis) against Ce-concentration inside the leaves of the plants grown on that medium (y-axis)

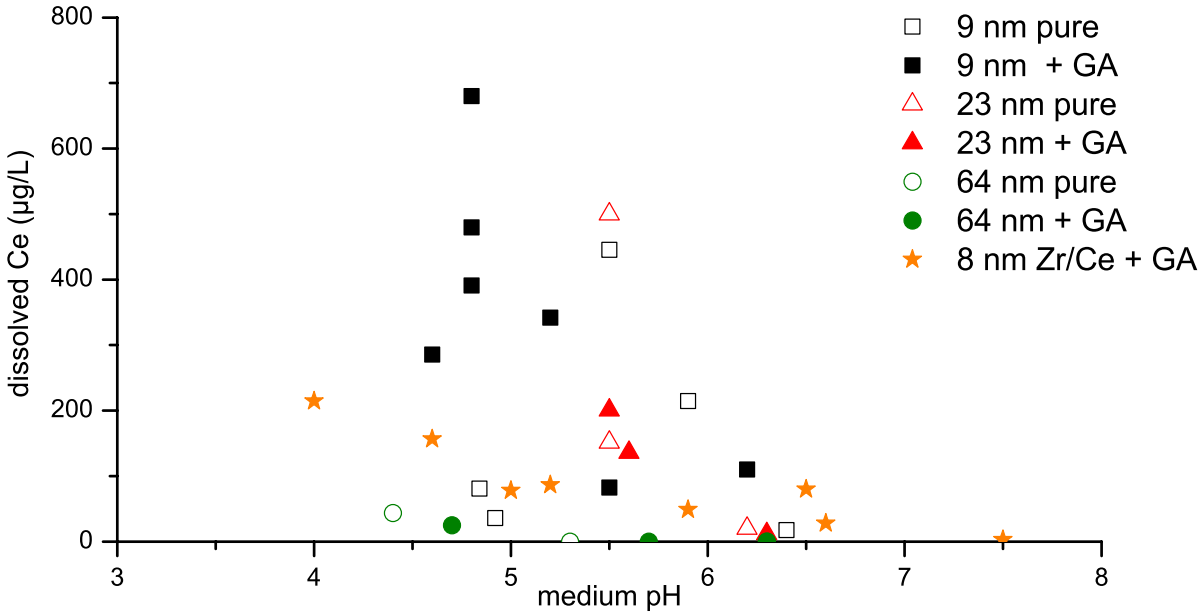

Fig. 5 Concentration of dissolved Ce in medium against the pH-value of medium on day 6. pH differences were induced by plant root growth/exudation.

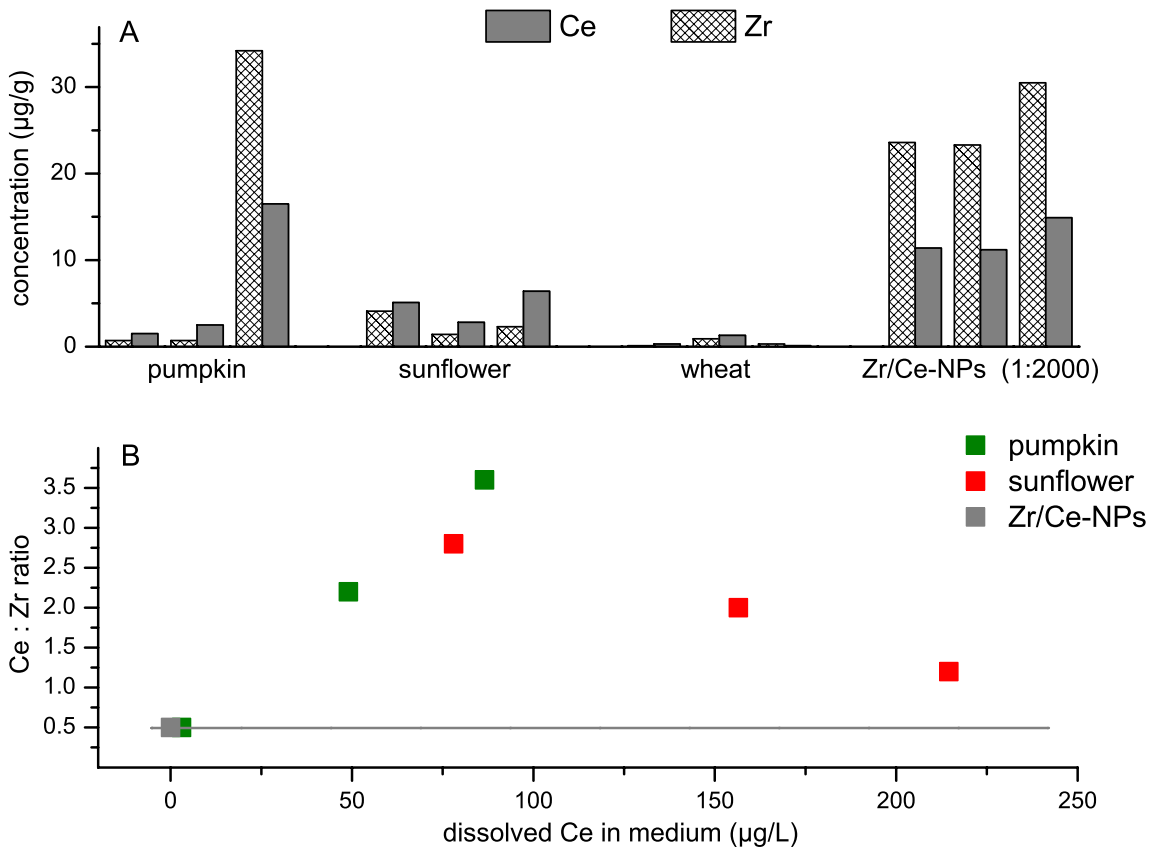

Fig. 6 Zr and Ce-concentration measured in plant leaves after Zr/CeO_x-NP-treatment. A) Concentration of Ce in leaves and NPs (diluted 1:2000) measured via ICP-MS after digestion using HF. Controls are not shown since values were below detection limit (0.2 µg/g). B) Plot of Ce:Zr-ratio measured in plant leaves against concentration of dissolved Ce in medium. The grey line indicates original ratio Ce:Zr of 0.5.

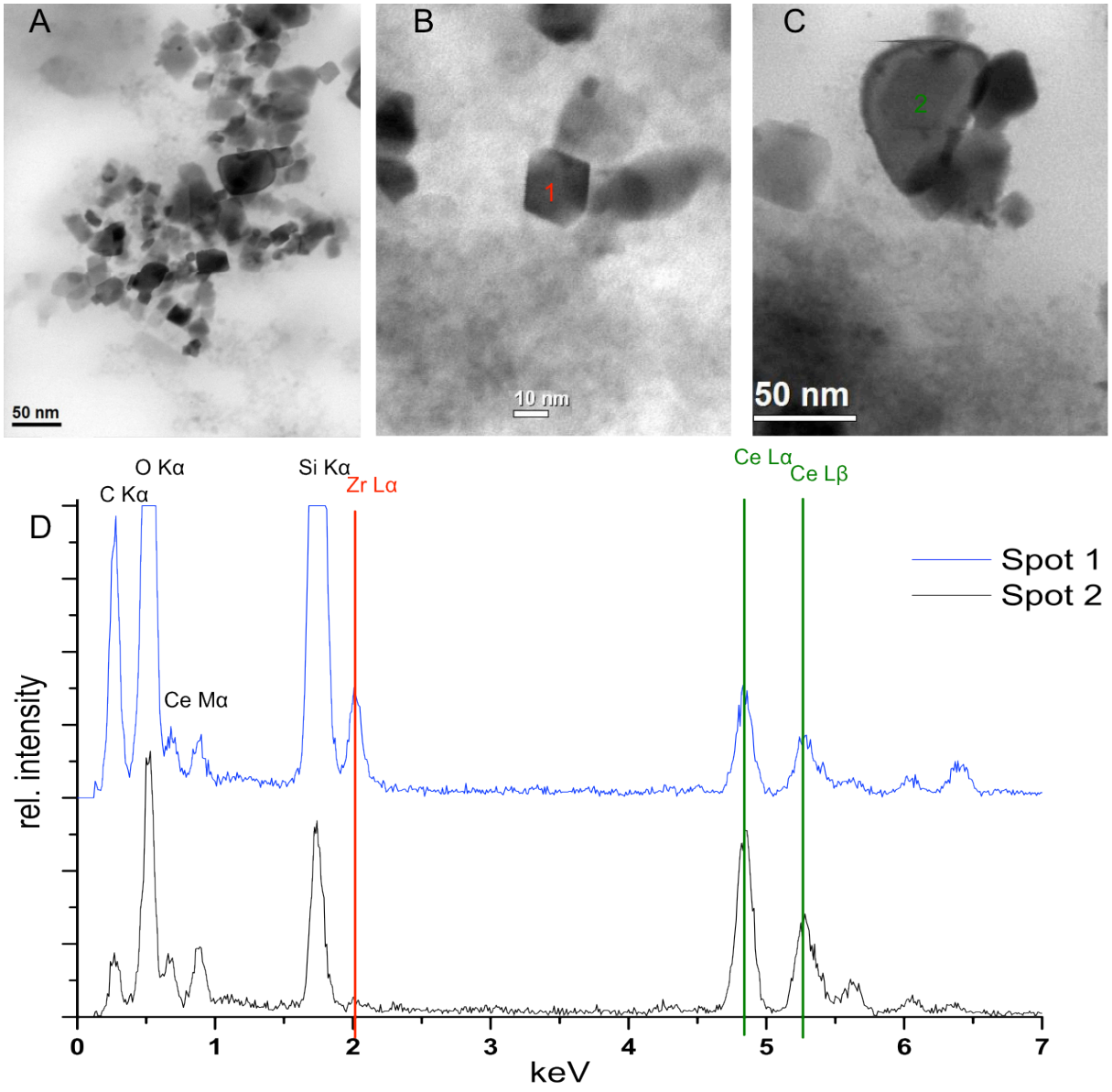

Fig. 7 STEM-EDX of NPs extracted from leaves of Zr/CeO_x treated sunflower. A) bright-field STEM image of NPs extracted from sunflower leaves; B) STEM image of rhombic NP in higher magnification. C)) STEM image of round-shaped NP; D) EDX- spectra of particles shown in 7B and 7C: the blue line represents particle 1, the black line represents particle 2 The peak at 2.0 keV marked with the red line represent Zr in sample and the peaks at 4.9 and 5.2 keV (green) represent Ce.